

## **Supplementary Material**

### **Aromatic Ring-flipping in Supercooled Water: Implications for NMR-based Structural Biology of Proteins**

Jack J. Skalicky, Jeffrey L. Mills, Surabhi Sharma and Thomas Szyperski\*

Department of Chemistry  
State University of New York at Buffalo  
Buffalo, NY 14260, USA

\*To whom correspondence should be addressed

## I. Extended Description of Materials and Methods

**Sample Preparation.** All NMR measurements were performed with 6 mM solutions of recrystallized BPTI (Sigma-Aldrich Co., MO; Cat. No. T 0256) at pH = 3.5 (for measurements in D<sub>2</sub>O, the uncorrected electrode reading was used to adjust pD). This pH was previously chosen for the high-quality NMR solution structure determination of BPTI.<sup>15</sup> Four NMR samples were prepared for the present study. “*sample I*”: with 90% H<sub>2</sub>O/ 10% D<sub>2</sub>O as the solvent using a 5 mm NMR tube (Wilmad, NJ; Cat. No. 528); “*sample II*”: with D<sub>2</sub>O as the solvent using a 5 mm NMR tube (Wilmad, NJ; Cat. No. 528); “*sample c1.7*”: with D<sub>2</sub>O as the solvent using three 1.7 mm o.d. glass capillary tubes<sup>2</sup> (Wilmad, NJ; Cat. No. 1365-1.7); “*sample c1.0*”: with D<sub>2</sub>O as the solvent using ten 1.0 mm o.d. glass capillary tubes (Wilmad, NJ; Cat. No. 1365-1.0). The capillaries for samples c1.7 and c1.0 were placed within a regular 5 mm NMR tube for measurements.<sup>2</sup> The resulting “filling factors”, *i.e.*, the volume filled with protein solution within the region assessed by the detection coil of the probe when compared with samples I and II, were, respectively, 0.41 and 0.28 for samples c1.0 and c1.7.

**NMR Spectroscopy.** NMR experiments were (i) recorded on Varian Inova 750 or Inova 600 spectrometers equipped with newest generation <sup>1</sup>H{<sup>13</sup>C,<sup>15</sup>N} probes, (ii) processed using the program PROSA,<sup>16</sup> and (iii) analyzed using the program XEASY.<sup>17</sup> Sample temperatures in the spectrometers were calibrated using the <sup>1</sup>H resonances of methanol that was filled in the same 5 mm, 1.7 mm or 1.0 mm tube arrangements as described above. Supercooling of NMR samples was monitored as described,<sup>2</sup> and 1D <sup>1</sup>H-NMR spectra were recorded at temperatures between  $T = 36\text{ }^{\circ}\text{C}$  and  $-16\text{ }^{\circ}\text{C}$  with  $t_{\text{max}} = 70\text{ ms}$ .

Eight 2D [<sup>1</sup>H,<sup>1</sup>H]-NOESY spectra<sup>10</sup> were recorded with a mixing time,  $\tau_{\text{mix}}$ , of 40 ms at 750 MHz <sup>1</sup>H spectrometer frequency and at  $T(\text{sample}) = -15\text{ }^{\circ}\text{C}$  (c1.0),  $-13\text{ }^{\circ}\text{C}$  (c1.7),  $-11\text{ }^{\circ}\text{C}$  (c1.7), -

9 °C (c1.7), -7 °C (c1.7), -5 °C (c1.7), -3 °C (c1.7) and 36 °C (c1.7). Between 256 (-15 °C) and 384 (36 °C) complex points were acquired along  $t_1$ , and between 425 (-15 °C) and 768 (36 °C) complex points were sampled along  $t_2$ . The corresponding maximal evolution times were:  $t_{1\max} = 34$  ms (-15 °C) and  $t_{1\max} = 52$  ms (36 °C), and  $t_{2\max} = 38$  ms (-15 °C) and  $t_{2\max} = 85$  ms (36 °C). For sequential resonance assignment, an additional NOESY spectrum ( $\tau_{\text{mix}} = 100$  ms) was recorded for sample I (*i.e.*, with 90% H<sub>2</sub>O/ 10% D<sub>2</sub>O as the solvent) at  $T = -6$  °C with 450( $t_1$ ) x 512( $t_2$ ) complex points ( $t_{1\max} = 53$  ms and  $t_{2\max} = 65$  ms). To allow for a direct comparison of relative cross peak intensities at the two temperatures  $T = -15$  and  $T = 36$  °C, two NOESY spectra were recorded in 18 and 36 hours, respectively, at 600 MHz for which  $\tau_{\text{mix}}$  was scaled with  $1/\tau_c$ , where  $\tau_c$  represents the correlation time for the overall rotational tumbling of BPTI (Figure 2).  $\tau_c(-15$  °C)  $\sim 12.5$  ns and  $\tau_c(36$  °C)  $\sim 3$  ns yielded  $\tau_{\text{mix}}(-15$  °C) = 15 ms and  $\tau_{\text{mix}}(36$  °C) = 70 ms, respectively. 300( $t_1$ ) x 400( $t_2$ ) complex points ( $t_{1\max} = 42$  ms and  $t_{2\max} = 55$  ms), and 400( $t_1$ ) x 512( $t_2$ ) complex points ( $t_{1\max} = 55$  ms and  $t_{2\max} = 71$  ms) were acquired at -15 °C and 36 °C, respectively. Prior to Fourier Transformation, the data were multiplied with a cosine function shifted by 15 degrees. The digital resolution after zero-filling was typically around 5 Hz/pt. along  $\omega_1$  and 0.6 Hz/pt. along  $\omega_2$ . The total measurement time for recording the NOESY spectra was 241 hours.

Three 2D [<sup>1</sup>H,<sup>1</sup>H]-TOCSY spectra<sup>10</sup> (sample c1.0; spin-lock r.f. field strength: 10 kHz) were recorded at a <sup>1</sup>H spectrometer frequency of 600 MHz and at  $T$  (sample) = -14.5 °C (c1.0) with  $\tau_{\text{mix}} = 38$  ms, and at  $T$  (c1.0) = -7.5 °C with  $\tau_{\text{mix}} = 38$  ms or 55 ms. 256 ( $t_1$ ) x 400 ( $t_2$ ) complex points ( $t_{1\max} = 39$  ms and  $t_{2\max} = 61$  ms) were acquired. Prior to Fourier Transformation, the data were multiplied with a cosine function shifted by 20 degrees. The digital resolution after zero-filling was 3.2 Hz/pt. along  $\omega_1$  and  $\omega_2$ . The total measurement time was 24 hours.

Eight series of three or four cross relaxation suppressed 2D [ $^1\text{H}$ ,  $^1\text{H}$ ]-EXSY spectra<sup>18</sup> were recorded, if not indicated otherwise, at 600 MHz  $^1\text{H}$  spectrometer frequency at  $T(\text{sample}) = -16.5$  °C (c1.0),  $-14.5$  °C (c1.0),  $-12.5$  °C (c1.0),  $-9.5$  °C (c1.7, 750 MHz),  $-9.5$  °C (c1.0),  $-7.5$  °C (c1.0),  $-5.5$  °C (c1.0), and  $-3.5$  °C (c1.0). Between 150 ( $-16.5$  °C) and 256 ( $-3.5$  °C) complex points were acquired along  $t_1$  and between 300 ( $-16.5$  °C) and 512 ( $-3.5$  °C) complex points were sampled along  $t_2$ , with  $t_{1\text{max}} = 14$  ms ( $-16.5$  °C) and  $t_{1\text{max}} = 24.0$  ms ( $-3.5$  °C), and  $t_{2\text{max}} = 38$  ms ( $-16.5$  °C) and  $t_{2\text{max}} = 56.8$  ms ( $-3.5$  °C). For each temperature, spectra with three or four different mixing times were recorded (10, 20, 30, 40 ms at  $T = -3.5, -5.5, -7.5, -9.5, -12.5$ ; 20, 30, 45 ms at  $T = -13.5$ ; 10, 20, 35 ms at  $T = -16.5$ , respectively). Prior to Fourier Transformation, the data were multiplied with a cosine function shifted by 10 degrees. The digital resolution after zero-filling was 4.4 Hz/pt. along both  $\omega_1$  and  $\omega_2$ . The total measurement time for recording the EXSY spectra was 192 hours.

2D [ $^{13}\text{C}$ ,  $^1\text{H}$ ]-HSQC spectra<sup>10</sup> were recorded with a  $^1\text{H}$ -spectrometer frequency of 750 MHz at  $T(\text{sample}) = -6$  °C (II) and  $25$  °C (II).  $51(t_1) \times 512(t_2)$  complex points were acquired, with  $t_{1\text{max}}(^{13}\text{C}) = 9.0$  ms and  $t_{2\text{max}}(^1\text{H}) = 56.8$  ms. Prior to Fourier Transformation, the data were multiplied by a cosine window shifted by 20 degrees. The digital resolution after zero-filling was 11.1 Hz/pt. along  $\omega_1$  and 4.4 Hz/pt. along  $\omega_2$ . The total measurement time to record the two spectra was 48 hours.

**Data Analysis.** All linear regression analyses were performed with the program SigmaPlot 4.0. The flipping rate,  $k_{\text{flip}}$ , of Phe 45 of BPTI was determined from both the 2D [ $^1\text{H}$ ,  $^1\text{H}$ ]-EXSY<sup>18</sup> and the 2D [ $^1\text{H}$ ,  $^1\text{H}$ ]-NOESY spectra.<sup>10</sup> In order to extract  $k_{\text{flip}}$  from EXSY with varying mixing times, the relation  $\ln[-2V_C/(V_C+V_D) + 1] = -2k_{\text{flip}}\tau_{\text{mix}}$  (eq. 1) was fitted by linear regression (which allows calculation of standard deviations from analytical expressions) to the experimental

data, where  $V_D$  and  $V_C$  represent the diagonal and cross peak volumes, respectively. Although the  $T_{1\rho}$ -relaxation times of the aromatic  $^1\text{H}^{\varepsilon/\delta}$  protons of Phe 45 ( $\sim 40$ -50 ms at  $-7.5^\circ\text{C}$ , as extracted from EXSY) are quite comparable to the mixing times (10-40 ms) used to record the EXSY spectra, accurate determination of  $k_{\text{flip}}$  was warranted because (i) the  $^1\text{H}^{\varepsilon/\delta}$   $T_{1\rho}$ -relaxation times of Phe 45 are all quite similar at  $T = -3.5^\circ\text{C}$  and below, a notion confirmed by line width analysis in NOESY (see Figure 8; note also that flip-broadening is negligible for  $^1\text{H}^{\varepsilon/\delta}$  of Phe 45 at  $T < -2^\circ\text{C}$ ) and because (ii) peak volumes,<sup>10</sup> and not intensities, were introduced into eq. 1. From NOESY,  $k_{\text{flip}}$  was determined for a given mixing time using the expression  $k_{\text{flip}} = [-1/(2\tau_{\text{mix}})] \cdot \ln[(\kappa-1)/(\kappa+1)]$  (eq. 2), where  $\kappa = V_D/V_C$ .

Eyring plots were obtained by fitting the Eyring equation<sup>19</sup> to the experimental data, *i.e.*,  $\Delta G^\ddagger/T = R \cdot \ln[k_B T/(h k_{\text{flip}})]$  (eq.3) *versus*  $1/T$ , where  $R$ ,  $k_B$  and  $h$  are the universal gas constant, Boltzmann's constant and Planck's constant, respectively. The activation enthalpy,  $\Delta H^\ddagger$ , and the activation entropy,  $\Delta S^\ddagger$ , are obtained from the slope and the inverse of the intercept, respectively. Ring flipping rates in supercooled water were predicted from activation parameters previously determined<sup>12,14</sup> at ambient  $T$  using  $1/k_{\text{flip}} = h/(k_B T) \cdot \exp[(\Delta H^\ddagger/RT - \Delta S^\ddagger/R)]$  (eq. 4). For the present study we further assumed that both  $\Delta H^\ddagger$  and  $\Delta S^\ddagger$  are independent of  $T$ .

**Correlation time for the overall rotational tumbling in supercooled water.** We have recently demonstrated<sup>2</sup> that hydrodynamic theory<sup>20</sup> allows accurate prediction of the correlation time of the overall rotational tumbling of globular proteins dissolved in supercooled water. In addition, previous  $^{13}\text{C}$  and  $^{15}\text{N}$  nuclear spin relaxation measurements<sup>21</sup> at ambient temperature showed that BPTI may be well approximated as a spherical molecule in the framework of hydrodynamic theory. We thus calculated the correlation time for the overall rotational tumbling of BPTI using the well established relation<sup>20a</sup>  $\tau_c = 4\pi[\eta(T)]r_H^3/3k_B T$  (eq. 5).  $r_H$  is the effective

radius with  $r_H = [3\bar{V}M/(4\pi N_A)]^{1/3} + r_w$ , where  $\bar{V} = 0.73 \text{ cm}^3/\text{g}$ ,  $M$ ,  $N_A$  and  $r_w$  are the protein's specific volume and molecular weight, Avogadro's number, and the added radius of a monolayer of water, respectively.<sup>20a</sup>

## II. Chemical Shift Tables

**Table S1.** Aromatic  $^1\text{H}$  chemical shifts<sup>a</sup> of BPTI

(a) in supercooled water at  $T = -15\text{ }^\circ\text{C}$

	$^1\text{H}^{\delta\text{x}}$	$^1\text{H}^{\delta\text{y}}$	QD	$^1\text{H}^{\epsilon\text{x}}$	$^1\text{H}^{\epsilon\text{y}}$	QE	$^1\text{H}^{\zeta}$
Phe 4			7.036			7.385	7.333
Tyr 10			7.352			7.111	
Tyr 21			6.731			6.903	
Phe 22			7.159			7.255	7.387
Tyr 23	7.247	7.157		6.304	6.359		
Phe 33			7.111			7.16	7.039
Tyr 35	6.718	7.832		7.009	6.817		
Phe 45	7.364	7.561		8.286	7.626		7.725

(b) at  $^{15}\text{ }T = 36^\circ\text{C}$

	$^1\text{H}^{\delta\text{x}}$	$^1\text{H}^{\delta\text{y}}$	QD	$^1\text{H}^{\epsilon\text{x}}$	$^1\text{H}^{\epsilon\text{y}}$	QE	$^1\text{H}^{\zeta}$
Phe 4			6.975			7.354	7.295
Tyr 10			7.31			7.076	
Tyr 21			6.705			6.763	
Phe 22			7.139			7.21	7.303
Tyr 23			7.146			6.316	
Phe 33			7.061			7.113	6.992
Tyr 35	6.661	7.748		6.906	6.755		
Phe 45							7.629

<sup>a</sup> in ppm relative to DSS.

**Table S2.** Methyl  $^1\text{H}$  and  $^{13}\text{C}$  chemical shifts<sup>a</sup> ( $\delta_{\text{DSS}}$ ) and  $\Delta\delta$  for BPTI at 36 and -7.5 °C.

Residue <sup>b</sup>	Atom <sup>c</sup>	$\delta^{13}\text{C}$ T=36°C	$\delta^{13}\text{C}$ T=-7.5°C	$\Delta\delta^{13}\text{C}$ ( $\delta_{36}-\delta_{-7.5}$ )	$\delta^1\text{H}$ T=36°C	$\delta^1\text{H}$ T=-7.5°C	$\Delta\delta^1\text{H}$ ( $\delta_{36}-\delta_{-7.5}$ )
Leu 6	$\text{C}^{\delta 1}(\text{H}^{\delta 1})_3$	22.9	23.0	-0.1	0.85	0.85	0.00
Leu 6	$\text{C}^{\delta 2}(\text{H}^{\delta 2})_3$	24.8	25.0	-0.2	0.94	0.93	0.01
Thr 11	$\text{C}^{\gamma 2}(\text{H}^{\gamma 2})_3$	21.2	21.1	0.1	1.37	1.38	-0.01
Ala 16	$\text{C}^{\beta}(\text{H}^{\beta})_3$	19.4	19.7	-0.3	1.16	1.18	-0.02
Ile 18	$\text{C}^{\gamma 2}(\text{H}^{\gamma 2})_3$	18.2	18.3	-0.1	0.96	0.96	0.00
Ile 18	$\text{C}^{\delta}(\text{H}^{\delta})_3$	13.9	14.2	-0.3	0.67	0.67	0.00
Ile 19	$\text{C}^{\gamma 2}(\text{H}^{\gamma 2})_3$	17.1	17.2	-0.1	0.70	0.70	0.00
Ile 19	$\text{C}^{\delta}(\text{H}^{\delta})_3$	10.5	10.6	-0.1	0.66	0.67	-0.01
Ala 25	$\text{C}^{\beta}(\text{H}^{\beta})_3$	18.9	18.9	0.0	1.55	1.53	0.02
Ala 27	$\text{C}^{\beta}(\text{H}^{\beta})_3$	20.1	19.7	0.4	1.17	1.18	-0.01
Leu 29	$\text{C}^{\delta 1}(\text{H}^{\delta 1})_3$	24.7	24.8	-0.1	0.74	0.73	0.01
Leu 29	$\text{C}^{\delta 2}(\text{H}^{\delta 2})_3$	24.6	24.6	0.0	0.84	0.85	-0.01
Thr 32	$\text{C}^{\gamma 2}(\text{H}^{\gamma 2})_3$	22.1	22.2	-0.1	0.57	0.59	-0.02
Val 34	$\text{C}^{\gamma 1}(\text{H}^{\gamma 1})_3$	21.1	21.1	0.0	0.79	0.79	0.00
Val 34	$\text{C}^{\gamma 2}(\text{H}^{\gamma 2})_3$	22.2	22.4	-0.2	0.69	0.68	0.01
Ala 40	$\text{C}^{\beta}(\text{H}^{\beta})_3$	19.6	19.7	-0.1	1.20	1.18	0.02
Ala 48	$\text{C}^{\beta}(\text{H}^{\beta})_3$	17.4	17.4	0.0	1.02	1.03	-0.01
Met 52	$\text{C}^{\epsilon}(\text{H}^{\epsilon})_3$	16.4	16.4	0.0	2.14	2.15	-0.01
Thr 54	$\text{C}^{\gamma 2}(\text{H}^{\gamma 2})_3$	22.2	22.5	-0.3	1.60	1.65	-0.05
Ala 58	$\text{C}^{\beta}(\text{H}^{\beta})_3$	19.5	19.2	0.3	1.31	1.31	0.00

<sup>a</sup>Chemical shifts are referenced relative to the methyl  $^1\text{H}$  resonance of DSS (Markley, J.L., Bax, A., Arata, Y., Hilbers, C.W., Kaptein, R., Sykes, B.D., Wright, P.E. and Wuthrich, K.J. *J. Biomol. NMR* 1998 **12**, 1-12). The reference sample contained 2 mM DSS in  $\text{H}_2\text{O}$  in a 1.7 mm o.d. glass capillary tube. The probe temperature was calibrated using methanol contained in a 1.7 mm o.d. glass capillary tube.

<sup>b</sup>Amino acid residues are given in three letter code.

<sup>c</sup>The nomenclature of the methyl carbon and proton atoms follows from that used in the BPTI chemical shift files named bmr45.str and bmr46.str deposited in the BioMagResBank.

**Table S3.** Amide  $^1\text{H}$  chemical shifts<sup>a</sup> ( $\delta_{\text{DSS}}$ ) and  $\Delta\delta$  for BPTI at 36, 0, and -7.5 °C.

Residue <sup>b</sup>	$\delta ^1\text{H}, sIII^c$ T=36 °C	$\delta ^1\text{H}, sIII^c$ T=0 °C	$\Delta\delta ^1\text{H}$ ( $\delta_{36}-\delta_0$ )	$\delta ^1\text{H}, sI^c$ T=0 °C	$\delta ^1\text{H}, sI^c$ T=0 °C	$\Delta\delta ^1\text{H}$ ( $\delta_0-\delta_{-7.5}$ )
Asp 3	8.64	8.90	-0.26	8.84	8.86	-0.02
Phe 4	7.80	8.05	-0.24	8.05	8.06	-0.01
Cys 5	7.43	7.55	-0.12	7.50	7.51	-0.01
Leu 6	7.56	7.68	-0.12	7.69	7.69	-0.01
Glu 7	7.51	7.59	-0.08	7.60	7.60	-0.01
Tyr 10	7.79	7.96	-0.17	7.97	7.97	-0.01
Thr 11	8.93	9.21	-0.28	9.20	9.24	-0.04
Gly 12	7.15	7.35	-0.21	7.34	7.36	-0.02
Cys 14	8.68	8.83	-0.15	8.84	8.86	-0.02
Lys 15	7.95	8.14	-0.19	8.14	8.18	-0.04
Ala 16	8.20	8.26	-0.06	8.26	8.26	0.00
Arg 17	8.18	8.47	-0.29	8.47	8.50	-0.03
Ile 18	8.11	8.24	-0.13	8.27	8.30	-0.04
Ile 19	8.67	8.95	-0.27	8.94	8.98	-0.04
Arg 20	8.38	8.48	-0.10	8.58	8.62	-0.04
Tyr 21	9.17	9.28	-0.11	9.30	9.30	-0.01
Phe 22	9.77	9.84	-0.08	9.84	9.85	-0.01
Tyr 23	10.54	10.66	-0.13	10.68	10.68	-0.01
Asn 24	7.75	7.75	0.00	7.78	7.79	-0.01
Ala 25	8.77	9.07	-0.30	9.01	9.05	-0.04
Lys 26	7.90	8.18	-0.28	8.05	8.06	-0.01
Ala 27	6.80	6.90	-0.10	6.89	6.90	-0.01
Gly 28	8.13	8.24	-0.11	8.24	8.25	-0.01
Leu 29	6.80	6.91	-0.10	6.93	6.93	-0.01
Cys 30	8.39	8.59	-0.20	8.59	8.62	-0.03
Gln 31	8.75	8.83	-0.08	8.76	8.78	-0.02
Thr 32	8.02	8.19	-0.17	8.20	8.20	0.00
Phe 33	9.35	9.42	-0.07	9.43	9.43	-0.01
Val 34	8.35	8.60	-0.25	8.59	8.62	-0.03

Tyr 35	9.38	9.56	-0.18	9.55	9.58	-0.03
Gly 36	8.60	8.76	-0.17	8.75	8.77	-0.02
Cys 38	7.75	7.79	-0.04	7.78	7.79	-0.01
Arg 39	9.05	9.27	-0.22	9.28	9.30	-0.03
Ala 40	7.37	7.50	-0.13	7.57	7.57	-0.01
Lys 41	8.31	8.44	-0.13	8.49	8.52	-0.03
Arg 42	8.35	8.61	-0.26	8.59	8.62	-0.03
Asn 43	7.21	7.26	-0.05	7.26	7.29	-0.03
Asn 44	6.76	6.84	-0.08	6.86	6.87	-0.01
Phe 45	9.92	10.04	-0.12	10.10	10.14	-0.04
Lys 46	9.91	10.15	-0.24	10.16	10.20	-0.04
Ser 47	7.46	7.50	-0.05	7.52	7.51	0.01
Ala 48	8.13	8.28	-0.15	8.29	8.29	-0.01
Glu 49	8.59	8.72	-0.13	8.66	8.67	-0.01
Asp 50	7.84	8.02	-0.18	7.98	7.99	-0.01
Cys 51	6.98	7.06	-0.08	7.08	7.08	-0.01
Met 52	8.58	8.69	-0.12	8.65	8.66	-0.01
Arg 53	8.26	8.30	-0.04	8.35	8.36	-0.01
Thr 54	7.39	7.47	-0.07	7.45	7.46	-0.01
Cys 55	8.23	8.42	-0.19	8.45	8.49	-0.04
Gly 56	7.95	8.16	-0.21	8.11	8.14	-0.04
Gly 57	8.18	8.46	-0.28	8.45	8.49	-0.04
Ala 58	7.92	8.24	-0.32	8.26	8.31	-0.04

<sup>a</sup>Chemical shifts are referenced relative to the methyl <sup>1</sup>H resonance of DSS (Markley, J.L., Bax, A., Arata, Y., Hilbers, C.W., Kaptein, R., Sykes, B.D., Wright, P.E. and Wuthrich, K.J. *J. Biomol. NMR* 1998 **12**, 1-12). The reference sample contained 2 mM DSS in H<sub>2</sub>O in a 1.7 mm o.d. glass capillary tube. The probe temperature was calibrated using methanol contained in a 1.7 mm o.d. glass capillary tube. The amide chemical shift thermal coefficients are all within the normal range of -1 and -9 ppb/°C.

<sup>b</sup>Amino acid residues are given in three letter code.

<sup>c</sup>*Sample I (sI)*: 6.0 mM BPTI, pH = 3.6 (see sample preparation above). *Sample III (sIII)*: 1.5 mM uniform <sup>15</sup>N-labeled BPTI, pH = 7 was kindly provided by Dr. G. Montelione, Rutgers University.

### III. Estimation of BPTI's cold denaturation melting temperature.

From Makhatadze et al. (1993) (Table 2, page 2031) we obtain that  $\Delta C_p$  for the unfolding transition of BPTI is between 2 and 3  $\text{kJ}\cdot\text{K}^{-1}\cdot\text{mol}^{-1}$ . Using equation (12) in Privalov (1990) (page 291), we then estimate that the cold denaturation melting temperature would be between 200 K and 236 K, respectively.

Privalov, P. L. (1990) Cold denaturation of proteins. *Crit. Rev. Biochem. Mol. Biol.* **25**, 282–305.

Makhatadze, G. I., Kim, K.-S., Woodward, C., Privalov, P. L. (1993) Thermodynamics of BPTI folding. *Protein Sci.* **2**, 2082–2036.

#### IV. Figures

**Figure S1.** Cross sections taken along  $\omega_1$  at  $\omega_2(^1\text{H}^{\text{ex}})$  of Phe 45 from 2D [ $^1\text{H}$ ,  $^1\text{H}$ ]-NOESY spectra ( $\tau_{\text{mix}} = 40$  ms) recorded between  $T = -3$  °C and  $-15$  °C. The position of the [ $\omega_1(^1\text{H}^{\text{ey}}), \omega_2(^1\text{H}^{\text{ex}})$ ] exchange cross peak is indicated with an arrow at the chemical shift of  $\text{H}^{\text{ey}}$  of Phe 45. The cross peak intensity reflects the ring flipping rate constant (Table 1), and the reduction of the exchange peak at the lower temperatures is apparent (see text). The cross peaks labeled with “1”, “2” and “3” are assigned to  $^1\text{H}^{\zeta}$ ,  $^1\text{H}^{\delta\text{y}}$  and  $^1\text{H}^{\delta\text{x}}$  of Phe 45, respectively. Chemical shifts are relative to DSS.

**Figure S2.** Temperature distribution for entries deposited in the BioMagResBank.<sup>24</sup> (A) For all entries comprising chemical shifts for Tyr and Phe ring protons. (B) For entries comprising non-degenerate chemical shifts for  $\text{H}^{\epsilon}$  and  $\text{H}^{\delta}$  pairs of Phe and Tyr. Note, the different scale in (B) reflecting the fact that the overwhelming majority of aromatic Tyr and Phe rings are flipping rapidly on the chemical shift time scale at ambient  $T$  (see text). Since most assignments were obtained in the framework of NMR structure determinations, the  $T$ -distribution of currently available NMR structures can be expected to be very similar.

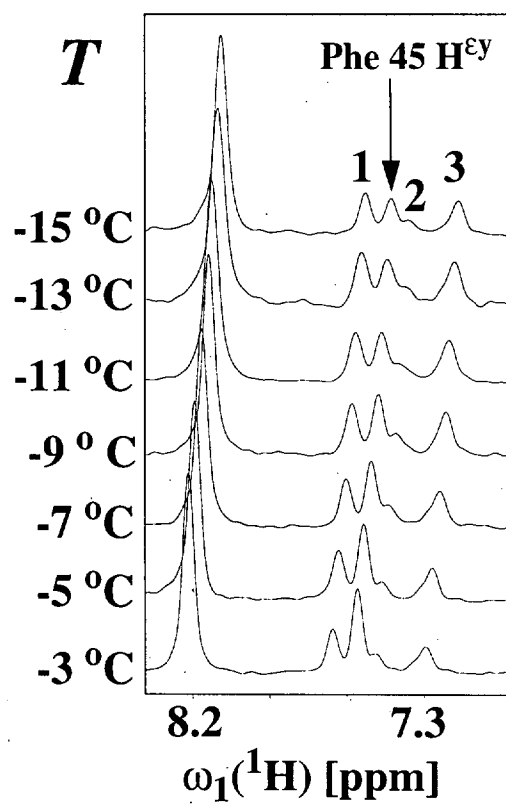


**Figure S1**

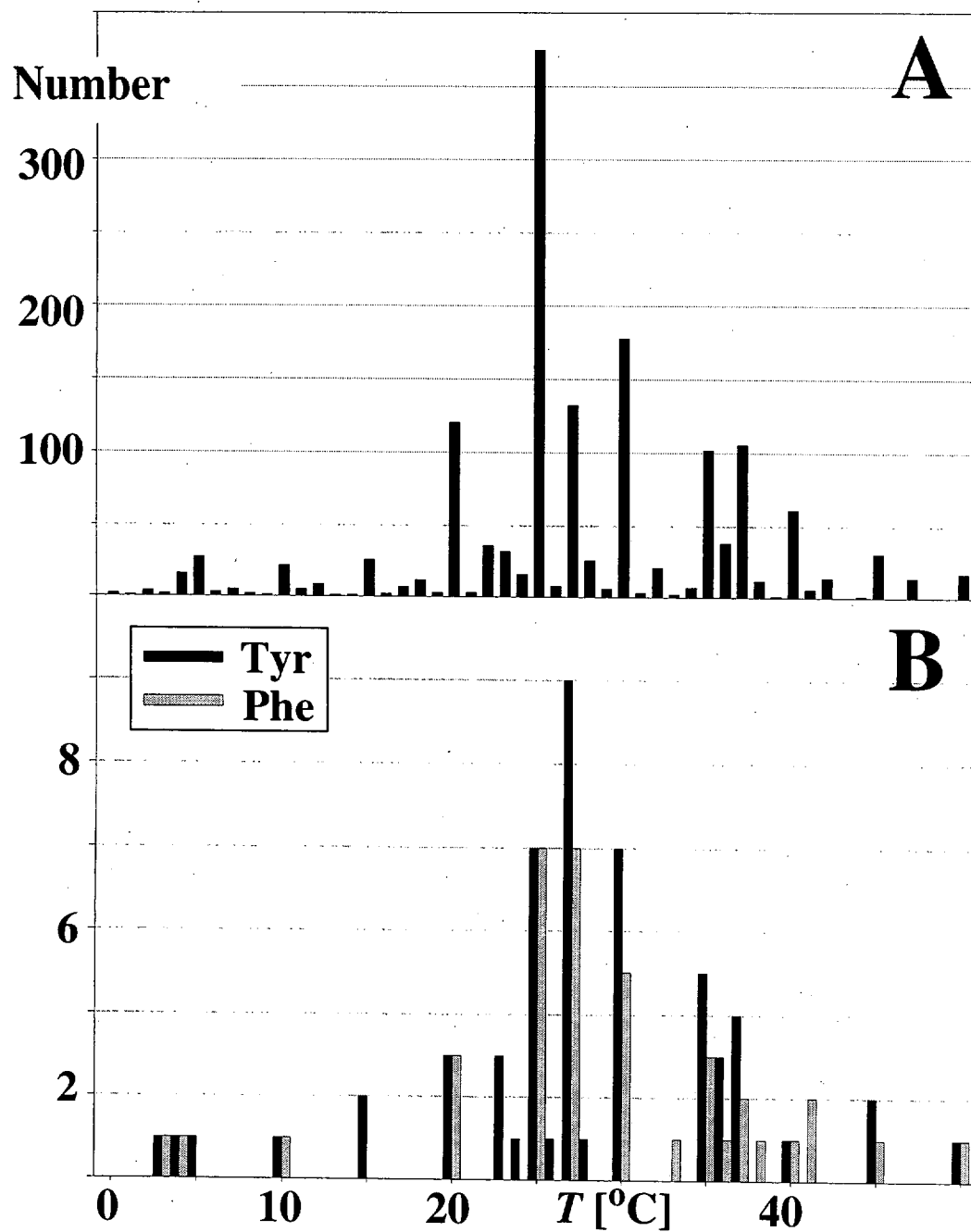


Figure S2